Shun-Jia Lin, Hong-Juan Sun*, Tong-Jiang Peng and Pei-Cao Wang

The adsorption kinetics and thermodynamics of cationic surfactants on graphite oxide

Abstract: The adsorption isotherms and structural evolution of alkyl quaternary ammonium bromide (C_nTAB) on graphite oxide (GO) were measured by means of an elemental analyzer, X-ray diffraction and Fourier transform infrared spectroscopy. In order to interpret the adsorption mechanism of surfactants onto GO, the adsorption kinetics and thermodynamics were further investigated. It was found that GO is a relatively efficient adsorbent within a wide range of temperatures (297–353 K), and the C_nTAB was intercalated and then agglomerated into the interlayer spacing of GO via ionic bonding and hydrophobic bonding. The saturation amount of alkyl ammonium adsorbed on GO was decreased with the rise in temperature, and the experimental data fitted well into the modified Langmuir (Langmuir-Freundlich) equation. In addition, the negative values of ΔG and ΔH showed that the adsorption process of C_nTAB onto the GO was spontaneous and exothermic.

Keywords: adsorption kinetics; adsorption thermodynamics; alkyl quaternary ammonium; graphite oxide.

***Corresponding author: Hong-Juan Sun,** Institute of Mineral Materials and Application, Southwest University of Science and Technology, Mianyang 621010, Sichuan, China, e-mail: sunhongjuan@swust.edu.cn
Shun-Jia Lin and Pei-Cao Wang: School of Science, Southwest University of Science and Technology, Mianyang 621010, Sichuan, China
Tong-Jiang Peng: Institute of Mineral Materials and Application, Southwest University of Science and Technology, Mianyang 621010, Sichuan, China

1 Introduction

Being a layered material, graphite oxide (GO) is considered to have large numbers of oxygen functional groups, such as hydroxyl (C-OH), carbonyl (C=O), carboxyl (COOH) and epoxy (C-O-C) groups [1, 2]. It is found that the hydroxyl and carboxyl groups are easily ionized in aqueous or alkaline solution, leading to a negatively charged property to the surface of GO. Owing to the existence of oxygen functional groups, GO can easily adsorb polar micromolecules or surfactants, forming an intercalation compound as a result. In recent years, adsorption of surfactants [3–9] onto GO has been extensively studied because of the exceptional adsorption property of GO, which can also be a promising adsorbent for organic pollutants as well as the precursor of graphene-based nanocomposites [5–7].

Nowadays, many different theoretical models have been proposed to characterize the adsorption process and adsorption mechanism of surfactants on solids, such as the Langmuir, Brunauer-Emmett-Teller (BET) and Freundlich isotherms [10–14]. Most of these models note that the molecules were adsorbed onto the surface of solids through van der Waals interactions, hydrophobic bonding, ionic bonding, charge transfer, etc. [15, 16]. Moreover, the well-known thermodynamic functions have also been investigated in order to interpret the adsorption mechanism [17, 18]. However, previous research was focused on the structural evolution of surfactant-intercalated GO, and the adsorption mechanism of surfactants onto GO was seldom reported. Hence, it is desirable to discuss the influence of adsorption temperature and thus obtain as much information as possible about the system from the most common source of adsorption isotherm data.

With the purpose of evaluating the adsorption mechanism, several cationic surfactants have been adsorbed by GO. In addition, in order to interpret the adsorption mechanism of alkyl quaternary ammonium bromide (C_nTAB) onto GO, the adsorption kinetics together with the thermodynamics and structural evolution were further investigated by elemental analyzer, X-ray diffraction (XRD) and Fourier transform infrared (FTIR) spectroscopy.

2 Materials and methods

2.1 Reagents and materials

Natural flake graphite, obtained from Qingdao Shenshu Graphite Manufacturing Plant, Qingdao, Shandong, China, was sieved through a 200-mesh sieve. The cationic surfactants used in this study were dodecyl trimethyl ammonium bromide (C_{12}TAB), tetradecyl trimethyl ammonium bromide (C_{14}TAB) and hexadecyl trimethyl ammonium bromide (C_{16}TAB), and were obtained from Chengdu Kelong Chem. Co., Ltd. (Sichuan, China). Other materials

and reagents, such as potassium permanganate ($KMnO_4$) and concentrated sulfuric acid (H_2SO_4), were chemically pure and purchased from Kelong Chem, Co., Ltd., China.

2.2 Preparation of C_nTAB/GO composites

GO was synthesized with natural flake graphite according to modified Hummers' method [19]. GO (0.2 g) was dissolved in 50 ml of 0.05 M NaOH and the mixture was evenly stirred in order to produce a GO suspension. Then, surfactants such as C_{12}TAB, C_{14}TAB and C_{16}TAB (dissolved in 50 ml of deionized water to obtain an aqueous solution) were added into the GO suspension and stirred for 1 h at different temperatures. The concentrations of added C_nTAB were 2.2, 3.3, 5.5, 11.0, 16.5, 22.0, 33.0 and 44.0 mM. The precipitate was filtered and then washed with deionized water to remove the residual C_nTAB and NaOH. After drying at 333 K overnight, C_nTAB/GO intercalation composite samples were obtained, marking C_n-GO-*t* (*n*=12, 14, 16; *t*=2.2, 3.3, 5.5, 11, 16.5, 22, 33, 44).

2.3 Instrumentation

Nitrogen content was measured by a Vario EL CUBE elemental analyzer (Elementar Analysensysteme GmbH, Germany) with 2 mg of sulfanilic acid as a reference. The amount adsorbed and the equilibrium concentration of surfactants were then calculated. XRD patterns were recorded on an X'pert Pro diffractometer (PANalytical B.V., The Netherlands) with Cu K_a radiation (40 kV and 40 mA in the continuous scanning range from 0.5° to 60°). FTIR spectra were recorded by a Nicolet 5700 infrared absorption spectrometer (Nicolet, USA) using KBr pellets. Raman spectra were recorded by an InVia spectrometer (Renishaw, UK) using a He-Ne laser operating at 514 nm.

3 Results and discussion

3.1 Adsorption kinetics

In order to evaluate the adsorption process of C_nTAB on GO, adsorption isotherms were plotted through measuring the nitrogen content of C_n-GO-*t* via elemental analyzer. Figure 1 shows the adsorption isotherms of C_{12}TAB, C_{14}TAB and C_{16}TAB on GO at different temperatures. It is found that the adsorption process of C_{12}TAB on GO is similar to that of C_{14}TAB and C_{16}TAB and can be divided into three stages. First, when the C_nTAB concentration is less than 5.5 mM, the adsorption amount of C_nTAB on GO is increased sharply with increasing equilibrium concentration. Second, the adsorption amount of C_nTAB on GO

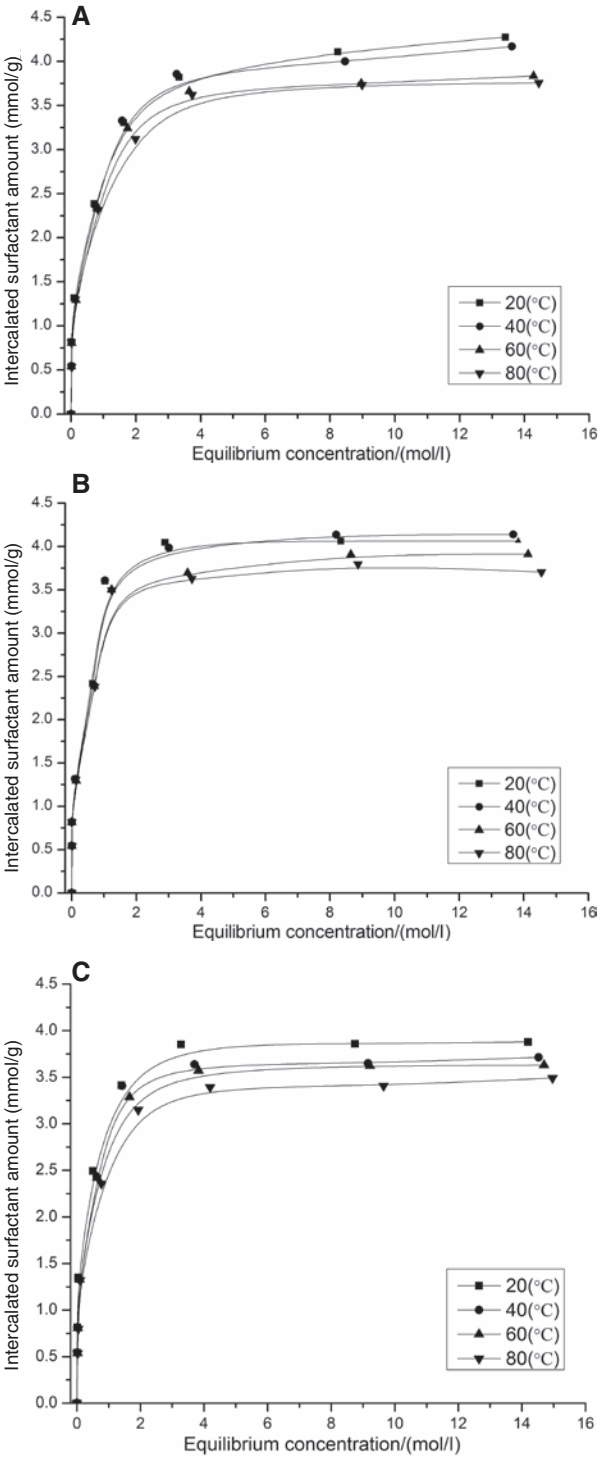

Figure 1 Adsorption isotherms of C_{12}TAB (A), C_{14}TAB (B) and C_{16}TAB (C) on GO at different temperatures.

is increased sluggishly when the C_nTAB concentration is increased from 5.5 to 16.5 mM. Finally, the saturated adsorption amount of C_nTAB is reached when the C_nTAB concentration is higher than 22.0 mM.

Experimental data of C_{12}TAB, C_{14}TAB and C_{16}TAB were fitted into the Freundlich, Langmuir, modified Langmuir (Langmuir-Freundlich) and BET isotherm equations. It was found that the experimental data fitted well into the nonlinear modified Langmuir isotherm equation, with correlation coefficients higher than 0.91 (Table 1). Furthermore, the experimental data of C_{12}TAB, C_{14}TAB and C_{16}TAB are in line with the linear regression equation $\Gamma=ac$ at low C_nTAB concentration (<5.5 mM), but are in line with the linear regression equation $\Gamma=bc+d$ at high C_nTAB concentration (from 5 to 16.5 mM). The parameter a is the parameter related to the ionic bonding force, and the parameters b and d are the hydrophobic bonding force and saturated adsorption amount via ionic bonding, respectively [12]. This indicated that the C_nTAB molecules are adsorbed onto the interlayer spacing of GO via ionic bonding under a low C_nTAB concentration, and the main driving force for the adsorption under a high C_nTAB concentration is hydrophobic bonding, which is weaker than the ionic bonding.

It was also found that the adsorption amount of C_nTAB on GO has little change while the temperature changed at a low C_nTAB concentration but has obvious reduction along with the rise in temperature at a high C_nTAB concentration. In pace with the temperature rising from 293 to 353 K, the saturated adsorption amounts of C_{12}TAB, C_{14}TAB and C_{16}TAB on GO are reduced from 4.065 to 3.705, 4.277 to 3757 and 3.879 to 3.493 mmol·g^{-1}, respectively (Table 1). This can be attributed to the solubility and desorption of C_nTAB. (1) Owing to the powerful force of ionic bonding, temperature has little influence on the adsorption amount of C_nTAB at low C_nTAB concentration. (2) At high C_nTAB concentration, the driving force changed to a powerless one (hydrophobic bonding); the Brownian motion of C_nTAB molecules was enhanced with the rise in temperature and thus increased the kinetic energy of C_nTAB molecules, consequently leading to a desorption of C_nTAB from GO. (3) Due to the rise in temperature, the interaction between C_nTAB molecules and water molecules intensified and led to a weaker adsorption tendency of C_nTAB onto GO [15, 20]. All of these led to the decrease in the saturated adsorption amount of C_nTAB on GO.

Table 1 Parameters of modified Langmuir equation fitted into the adsorption isotherms of C_nTAB on GO at different temperatures.

Surfactants	T (K)	Γ_∞ (mmol·g^{-1})	Modified Langmuir equation		
			k (l·mol^{-1})	R^2	n
C_{12}TAB	293	4.065	3.720	0.917	0.831
	313	4.123	3.366	0.912	0.828
	333	3.913	3.269	0.912	0.901
	353	3.705	–	–	–
C_{14}TAB	293	4.277	2.338	0.941	0.700
	313	4.171	2.445	0.953	0.728
	333	3.836	2.717	0.963	0.778
	353	3.757	2.711	0.951	0.766
C_{16}TAB	293	3.879	4.702	0.973	0.720
	313	3.714	4.199	0.966	0.749
	333	3.629	4.325	0.979	0.832
	353	3.493	3.782	0.985	0.824

3.2 Adsorption thermodynamics

The thermodynamic parameters can be obtained by using the thermodynamic equations (1)–(3) [13, 14].

$$\ln K_d = \Delta S / R - \Delta H / RT \quad (1)$$

$$\Delta G = \Delta H - T\Delta S \quad (2)$$

$$K_d = \Gamma / c. \quad (3)$$

ΔG is Gibbs free energy change of the adsorption process, and ΔH and ΔS are the enthalpy change and entropy change of the adsorption process, respectively. The thermodynamic parameters of the adsorption process of C_{12}TAB, C_{14}TAB and C_{16}TAB onto GO at various concentrations and different temperatures are shown in Table 2.

The negative values of ΔH in different C_nTAB concentrations are an indication of an exothermic adsorption process. It is obvious that the rise in temperature will hinder the adsorption. The value of ΔH is also appropriate to determine the molecules' interactions in the adsorption process. As introduced by Oepen et al. [21], the measured energies of each interaction are as follows: van der Waals interaction, 4–9 kJ·mol^{-1}; hydrophobic bonding, 4 kJ·mol^{-1}; hydrogen bonding, 2–40 kJ·mol^{-1}; and chemisorptions, 62–84 kJ·mol^{-1}. The absolute value of ΔH in the adsorption of C_{12}TAB amounts to 1.76–6.96 kJ·mol^{-1}, and those of C_{14}TAB and C_{16}TAB amount to 2.15–28.54 and 2.18–18.83 kJ·mol^{-1}, respectively. This indicated that the driving forces of the adsorption process include ionic bonding, hydrophobic bonding and hydrogen bonding.

In addition, ΔG reflects the driving force of the adsorption process. As shown in Table 2, the negative value of ΔG indicates that C_nTAB molecules are adsorbed onto GO spontaneously, and the values of ΔS, which indicate the degree of confusion in the random motion of microscopic

Table 2 Thermodynamic parameters for the absorption of the surfactants on GO in various concentrations and at different temperatures.

Surfactant	Concentration (mM)	ΔH (kJ·mol^{-1})	ΔS (kJ·K^{-1}·mol^{-1})	ΔG (kJ·mol^{-1})			
				293 K	313 K	333 K	353 K
C_{12}TAB	2.2	-6.96	69.66	-27.39	-28.78	-30.17	-31.57
	3.3	-4.28	90.39	-30.77	-32.57	-34.38	-36.19
	5.5	-3.18	67.34	-22.91	-24.25	-25.60	-26.95
	11.0	-1.76	62.34	-20.03	-21.27	-22.52	-23.77
	16.5	-3.70	55.43	-19.94	-21.05	-22.16	-23.27
	22.0	-5.77	40.78	-17.72	-18.53	-19.35	-20.16
	33.0	-2.12	44.51	-15.16	-16.05	-16.94	-17.83
	44.0	-2.17	40.14	-13.93	-14.73	-15.54	-16.34
C_{14}TAB	2.2	-8.72	59.25	-26.08	-27.26	-28.45	-29.64
	3.3	-28.54	6.19	-30.36	-30.48	-30.60	-30.73
	5.5	-5.89	58.42	-23.01	-24.18	-25.35	-26.52
	11.0	-2.77	58.03	-19.77	-20.93	-22.09	-23.25
	16.5	-3.84	50.70	-18.70	-19.71	-20.73	-21.74
	22.0	-2.81	49.26	-17.24	-18.23	-19.21	-20.20
	33.0	-3.12	41.81	-15.36	-16.20	-17.04	-17.87
	44.0	-3.20	37.12	-14.07	-14.81	-15.56	-16.30
C_{16}TAB	2.2	-12.10	47.26	-25.95	-26.89	-27.84	-28.78
	3.3	-18.83	29.76	-27.55	-28.14	-28.74	-29.33
	5.5	-12.11	44.05	-25.02	-25.90	-26.78	-27.66
	11.0	-6.52	48.46	-20.72	-21.69	-22.65	-23.62
	16.5	-5.85	45.28	-19.12	-20.03	-20.93	-21.84
	22.0	-5.04	41.46	-17.19	-18.02	-18.84	-19.67
	33.0	-2.92	40.64	-14.82	-15.64	-16.45	-17.26
	44.0	-2.18	39.17	-13.66	-14.44	-15.23	-16.01

particles, are decreased along with the increase in C_nTAB concentration. This can be interpreted by the further filling and agglomeration of C_nTAB in the interlayer spacing of GO, thus decreasing the degrees of freedom of motion of the C_nTAB molecules.

Furthermore, increasing the C_nTAB concentration will also lead to fewer negative values of ΔH. This indicated that the driving forces of adsorption changed from a strong one (ionic bonding) to a weak one (hydrophobic bonding). In addition, decreasing the force will weaken

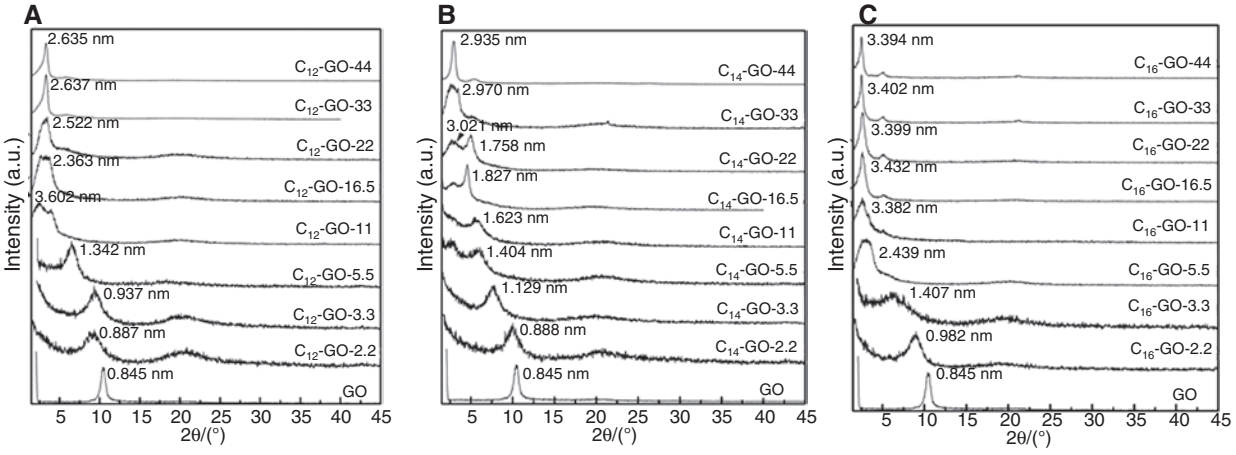

Figure 2 XRD patterns of GO and series of C_{12}-GO-*t* (A), C_{14}-GO-*t* (B) and C_{16}-GO-*t* (C).

the spontaneity of the adsorption process, consequently leading to a less negative value of ΔG.

3.3 Formation of C_nTAB/GO composites

In order to confirm the adsorption kinetics and thermodynamics of C_nTAB absorbed onto GO, XRD and FTIR spectroscopy were used to investigate the formation of C_nTAB/GO composites. Figure 2 shows the XRD patterns of GO together with C_nTAB/GO prepared in different concentrations of C_{12}TAB, C_{14}TAB and C_{16}TAB at 293 K. The diffraction peak of GO gradually shifts toward the lower angle with the increase in C_nTAB concentration, indicating that the C_nTAB molecules are intercalated into the interlayer spacing of GO, leading to an expansion of GO layer spacing. However, the diffraction peaks of intercalation composites become more diffuse than that of GO under a low C_nTAB concentration but become sharper with increasing C_nTAB concentration. This indicated that at low C_nTAB concentration, the low packing density of C_nTAB on GO will lead to the random distribution of C_nTAB into the interlayer spacing of GO, representing a disordered stacking of GO layers. The packing density of C_nTAB into GO was increased with the increase in C_nTAB concentration, thus leading to regular distribution and aggregation of C_nTAB into the interlayer spacing of GO. It is noteworthy that the two diffraction peaks of the C_{14}TAB-GO-22 sample can be assigned to different arrangement models of C_{14}TAB into the GO layer.

Figure 3 shows the FTIR spectra of GO and series of C_{16}-GO-*t*. The peaks at 3390, 1722, and 1400–1095 cm^{-1} for GO are attributed to the OH, C=O in COOH and C-O in C-OH/C-O-C (epoxy) functional groups, respectively [22]. Compared with the peaks of GO, the peaks at 1722 and 1400–1095 cm^{-1} for C_{16}-GO-*t* disappeared along with the increase in C_{16}TAB concentration. These indicate that the cationic surfactants with positive charge are ionically bonded to COO^- and CO^- groups of GO. Those at 2917, 2850 and 1473 cm^{-1} assigned to intercalated surfactant appeared when C_{16}TAB molecules were inserted into the interlayer spacing of GO. Moreover, the peak at 2917 cm^{-1} of C_{16}TAB is blue-shifted to 2920 cm^{-1}, and the peak at 1473 cm^{-1} red-shifted to 1466 cm^{-1}. These prove that in pace with the increase in C_{16}TAB concentration, the conformation of C_{16}TAB molecules is becoming more ordered and aggregated in the interlayer spacing of GO [23].

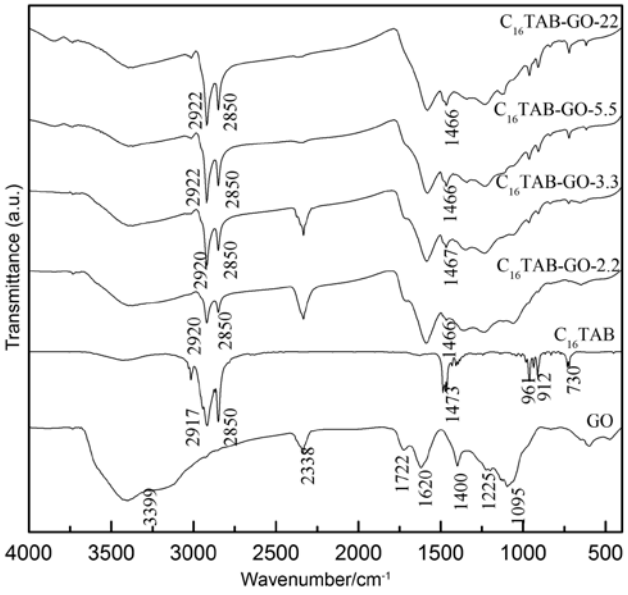

Figure 3 FTIR spectra of GO and series of C_{16}-GO-*t*.

4 Conclusion

In this study, the adsorption isotherms of C_nTAB on GO have been obtained and fitted well into the modified Langmuir equations. The adsorption mechanism of C_nTAB on GO was interpreted by the adsorption kinetics and thermodynamics, which were obtained from the studies of adsorption isotherms at different temperatures.

On the basis of the adsorption kinetics and thermodynamics, the C_nTAB molecules were intercalated into the interlayer spacing of GO via ionic bonding and hydrophobic bonding, and then further filled and agglomerated in the interlayer spacing of GO. Owing to the powerful force of ion bonding, temperature has little influence on the adsorption amount of C_nTAB at low C_nTAB concentration but has a large influence at high C_nTAB concentration. In addition, the adsorption process of C_nTAB onto the GO is spontaneous and exothermic.

Acknowledgments: This work was financially supported by the National Natural Science Foundation of China (Grant No. 41272051), the Doctoral Fund of Southwest University of Science and Technology (Grant No. 11ZX7135) and the Graduate Innovation Fund of Southwest University of Science and Technology (Grant No. 13ycjj49).

Received October 6, 2013; accepted March 23, 2014; previously published online May 20, 2014

References

[1] Stankovich S, Dikin DA, Ruoff RS. *Carbon* 2007, 45, 1558–1565.
[2] Nethravathi C, Rajamathi M. *Carbon* 2008, 46, 1994–1998.
[3] Liang YY, Wu DQ, Mullen K. *Adv. Mater.* 2009, 21, 1679–1683.
[4] Vadukumpully S, Paul J, Valiyaveettil S. *Carbon* 2009, 47, 3288–3294.
[5] Matsuo Y, Watanabe K, Sugie Y. *Carbon* 2003, 41, 1545–1550.
[6] Ramesha GK, Kumara AV, Sampath S. *J. Colloid Interface Sci.* 2011, 361, 270–277.
[7] Matsuo Y, Higashika S, Sugie Y. *J. Mater. Chem.* 2002, 12, 1592–1596.
[8] Hang ZD, Wang JQ. *J. Inorg. Chem.* 2003, 5, 459–461.
[9] Matsuo Y, Niwa T, Sugie YP. *Carbon* 1999, 37, 897–901.
[10] Xu SH, Boyd SA. *Environ. Sci. Technol.* 1995, 29, 3022–3028.
[11] Lee SY, Cho WJ, Lee M. *J Colloid Interface Sci.* 2005, 284, 667–673.
[12] Chen BL, Mao JF, Lv SF. *Chem. J. Chin. Universities* 2009, 30, 1830–1834.
[13] Xu S, Sheng G, Boyd SA. *Adv. Agron.* 1997, 59, 25–62.
[14] Ghiaci M, Kalbasi RJ, Shariatmadari H. *J. Chem. Thermodyn.* 2004, 36, 707–713.
[15] Zhao GX. *Physico-Chemistry of Surfactant*, Peking University Press: Peking, 1991, pp 105–109.
[16] He HP, Ray F, Bostrom T. *Appl. Clay Sci.* 2006, 31, 262–271.
[17] Ghiaci M, Kia R, Kalbasi RJ. *J. Chem. Thermodyn.* 2004, 36, 95–100.
[18] Ghiaci M, Kalbasi RJ, Abbaspour A. *Colloids Surf., A* 2007, 297, 105–113.
[19] Yang YH, Sun HJ, Peng TJ. *J. Inorg. Chem.* 2011, 26, 2083–2090.
[20] Teng XR. *Surface Physical Chemistry*, Chemical Industry Press: Peking, 2009, pp 96–101.
[21] Oepen BV, Kordel W, Klein W. *Chemosphere* 1991, 22, 285–304.
[22] Titelman GI, Gelman V, Bron S, Khalfin RL, Cohen Y, Peled HB. *Carbon* 2005, 43, 641.
[23] Vaia RA, Teukolsky RK, Giannelis EP. *Chem. Mater.* 1994, 6, 1017–1022.